



# Differences in Staining for Neutrophil Elastase and its Controlling Inhibitor SLPI Reveal Heterogeneity among Neutrophils in Psoriasis

Joanna Skrzeczynska-Moncznik<sup>1</sup>, Katarzyna Zabieglo<sup>1</sup>, Oktawia Osiecka<sup>1</sup>, Agnieszka Morytko<sup>1</sup>, Piotr Brzoza<sup>1</sup>, Lukasz Drozd<sup>1</sup>, Monika Kapinska-Mrowiecka<sup>2</sup>, Brice Korkmaz<sup>3</sup>, Maciej Pastuszcak<sup>4,5</sup>, Joanna Kosalka-Wegiel<sup>5</sup>, Jacek Musial<sup>5</sup> and Joanna Cichy<sup>1</sup>

Neutrophils are broadly classified into conventional neutrophils (PMNs) and low-density granulocytes (LDGs). LDGs are better than PMNs at generating neutrophil extracellular traps (NETs), which may contribute to the pathology of autoimmune diseases. We hypothesized that LDGs and PMNs differ in their levels of unrestrained NE that supports NET generation. Here, we show that individuals with psoriasis contain elevated levels of LDGs and that in contrast to PMNs, the LDGs display higher staining for NE and lower staining for its inhibitor SLPI. The heterogeneity between blood-derived LDGs and PMNs was somewhat reminiscent of the differences in the NE and SLPI staining patterns observed in psoriasis skin-infiltrating neutrophils. Distinctive staining for NE and SLPI in LDGs and PMNs did not result from differences in their protein levels nor manifested in higher total proteolytic activity of NE in LDGs; rather, it likely depended on different cytosolic sequestration of these proteins. The disparate profile of NE and SLPI in LDGs and PMNs coincided with altered migratory responses of these cells to cutaneous chemoattractants. Collectively, differential NE and SLPI staining identifies common attributes of both circulating and skin-infiltrating neutrophils, which may guide neutrophil migration to distinct skin regions and determine the localization of LDGs-mediated cutaneous pathology.

*Journal of Investigative Dermatology* (2020) **140**, 1371–1378; doi:10.1016/j.jid.2019.12.015

## INTRODUCTION

The infiltration of the skin by neutrophils is one of the hallmarks of psoriasis. Neutrophils can contribute to skin inflammation via different means: as a source of IL-17 (Lin et al., 2011), through the activation of the IL-36 family of cytokines by proteolytic processing (Henry et al., 2016), via the release of neutrophil extracellular traps (NETs) and stimulation of plasmacytoid dendritic cells (Lande et al., 2011; Skrzeczynska-Moncznik et al., 2012) or through NETs-mediated induction and/or expansion of memory T helper type 17 cells (Lambert et al., 2019).

NETs are DNA deposits decorated by nuclear and cytoplasmic-derived proteins. NE contributes to NET

formation through histone processing, leading to chromatin decondensation (Papayannopoulos et al., 2010). The proteolytic activity of NE is controlled by endogenous inhibitors, such as SLPI, (Majchrzak-Gorecka et al., 2016). SLPI is the major inhibitor of NE present in the neutrophil cytosol and blunts both histone processing and NET expulsion into the extracellular space (Zabieglo et al., 2015).

At least two populations of circulating neutrophils have been described in humans: low-density granulocytes (LDGs) and conventional polymorphonuclear neutrophils (PMNs). Whereas PMNs sediment together with red blood cells during density gradient separations, LDGs localize to the peripheral blood mononuclear cell (PBMC) fraction (Carmona-Rivera and Kaplan, 2013). LDGs were first described in patients with systemic lupus erythematosus (SLE), where they were found to be enriched in transcripts that encode proteins found in the early stages of neutrophil differentiation (Bennett et al., 2003; Villanueva et al., 2011) and to contain non-lobulated and hyposegmented nuclei, unlike PMNs (Carmona-Rivera and Kaplan, 2013). These findings suggest that LDGs are newly emergent neutrophils that are mobilized from the bone marrow to circulation before they are terminally differentiated. However, the immature phenotype of LDGs is not consistent with the cell surface molecule expression on these cells, which is more typical of fully-developed neutrophils (Carmona-Rivera and Kaplan, 2013). The lower buoyancy of LDGs may also be the result of cell activation that is often associated with a decrease in cell content owing

<sup>1</sup>Department of Immunology, Faculty of Biochemistry, Biophysics and Biotechnology, Jagiellonian University, Kraków, Poland; <sup>2</sup>Department of Dermatology, Zeromski Hospital, Kraków, Poland; <sup>3</sup>INSERM (National Institute for Medical Research) U-1100, "The Research Center for Respiratory Diseases" and The University of Tours, Tours, France;

<sup>4</sup>Department of Dermatology, Jagiellonian University Medical College, Kraków, Poland; and <sup>5</sup>Department of Medicine, Jagiellonian University Medical College, Kraków, Poland

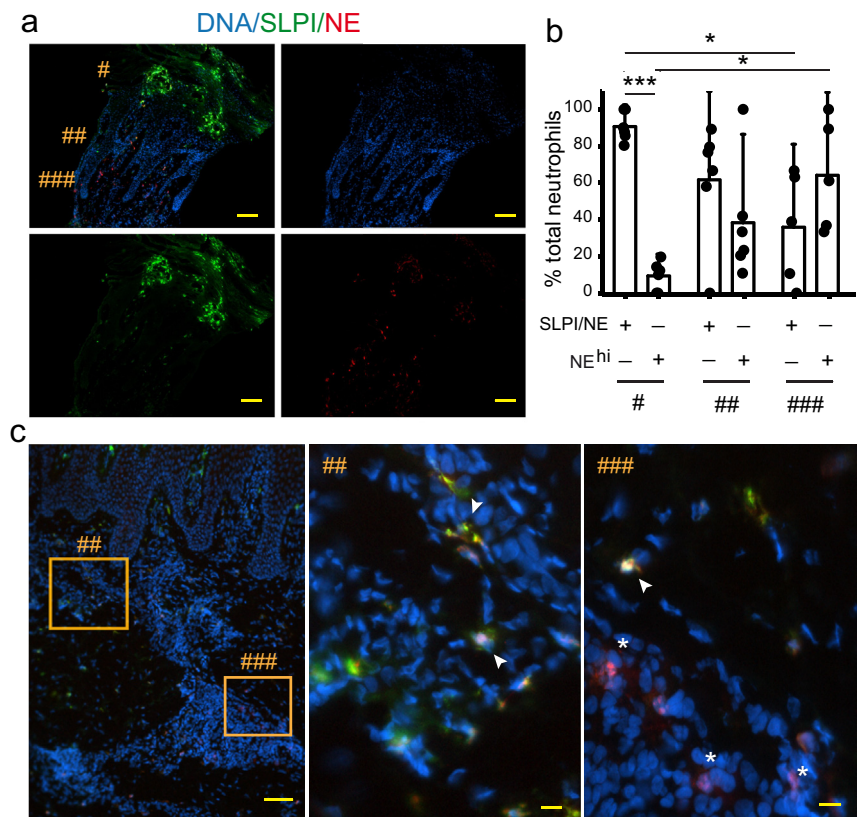
Correspondence: Joanna Cichy, Faculty of Biochemistry, Biophysics and Biotechnology, Jagiellonian University, Gronostajowa 7 Street, 30-387 Krakow, Poland. E-mail: [Joanna.Cichy@uj.edu.pl](mailto:Joanna.Cichy@uj.edu.pl)

Abbreviations: Ab, antibody; fMLP, N-formylmethionyl-leucyl-phenylalanine; LDG, low-density granulocyte; NET, neutrophil extracellular trap; PBMC, peripheral blood mononuclear cell; PMN, polymorphonuclear neutrophil; SLE, systemic lupus erythematosus

Received 31 July 2019; revised 17 December 2019; accepted 30 December 2019; accepted manuscript published online 13 January 2020; corrected proof published online 13 February 2020

**Figure 1. Neutrophils infiltrating the skin of patients with psoriasis differ in their pattern of NE and SLPI staining.**

Fluorescence microscopy images of lesional skin stained for NE (red), SLPI (green), and DNA (blue). Indicated skin regions (#, ##, ###) represent epidermis, upper dermis, and lower dermis, respectively. (a) An overlay or single channel images from one donor. (b) Analysis of the distribution of neutrophils in regions “# - ###” based on the indicated NE and SLPI staining pattern,  $n = 6$ . For each patient, at least six different high-power fields spanning the epidermis and dermis were analyzed. Each data point represents one experiment, and bars indicate the mean value  $\pm$  standard deviation in each group. \*\*\* $P < 0.001$ , \* $P < 0.05$  by an analysis of variance followed by a Tukey post hoc test. (c) Overlay image from a second donor with enlarged regions ## and ### demonstrating neutrophils that differ in staining for NE and SLPI. Neutrophils that are positive primarily for NE (NE<sup>hi</sup>) are shown by asterisks. Arrowheads highlight neutrophils that stained strongly for both NE and SLPI (SLPI/NE). Bar = 100  $\mu$ m (a, c left panel) or 10  $\mu$ m (c middle and right panels).



to degranulation (Hacbarth and Kajdacsy-Balla, 1986) and/or other alterations, such as an increase in cell volume (Sagiv et al., 2015). LDGs may represent a heterologous population of both immature and mature (either activated, aged, or primed) neutrophils (Nicolás-Ávila et al., 2017).

Patients with autoimmune diseases, such as SLE and psoriasis, upregulate the levels of circulating LDGs; this is notable, as LDGs counts are associated with the severity of psoriasis (Teague et al., 2019). Moreover, in autoimmune patients, LDGs display pro-inflammatory potential, such as toxicity to endothelial cells and a heightened ability to synthesize tumor necrosis factor- $\alpha$  or IFNs (Denny et al., 2010). Although these data suggest that LDGs might promote autoimmune conditions, studies of these cells are hampered by the lack of specific phenotypic and functional markers. Therefore, a better knowledge of neutrophil heterogeneity may provide important insights into the functional diversity of these cells.

## RESULTS

### Neutrophils from psoriasis patients are phenotypically and functionally diverse

To determine whether the neutrophils infiltrating skin of psoriasis patients differ in immunoreactivity for NE and/or SLPI, we stained skin samples of these patients with anti-NE and anti-SLPI antibodies (Abs), followed by fluorescence microscopy. Skin samples derived from the same donors exhibited different staining patterns, manifested by NE and SLPI costaining (SLPI/NE), or staining predominantly for NE (NE<sup>hi</sup>) (Figure 1a–c). Whereas neutrophils that costained for

NE and SLPI were the most abundant in the epidermis, neutrophils with stronger staining for NE were mostly seen in deeper skin regions (Figure 1b and c). Thus, neutrophils that infiltrate diverse skin niches are heterogenous in respect to NE and SLPI staining.

Different populations of circulating neutrophils may account for neutrophil heterogeneity in psoriasis skin. To determine whether LDGs and PMNs differ in NE and/or SLPI staining, we next analyzed the frequency and phenotype of these two populations isolated from the peripheral blood of psoriasis patients and healthy individuals by flow cytometry. SLE patients served as the positive control. In agreement with previous reports (Lin et al., 2011; Teague et al., 2019), we found higher levels of LDGs in PBMCs from psoriasis and SLE patients than those from healthy individuals. PBMCs from psoriasis donors showed 5-fold higher levels of LDGs on average, which constituted as high as 14–18% of the total PBMCs in some patients (Figure 2a and b).

Several surface markers have been previously studied with respect to the status of LDGs. These include markers of mature neutrophils, such as CD10, or those of activated neutrophils that upregulate CD66b and CD11b and downregulate CD62L surface levels (Scapini et al., 2016). We found that LDGs from psoriasis donors did not exhibit significant alterations in the surface expression of CD10 and CD11b but expressed significantly higher levels of CD15 and CD66b and lower levels of CD62L, in contrast to PMNs (Figure 2c). The profile was consistent with a mature neutrophil phenotype and indicated some level of

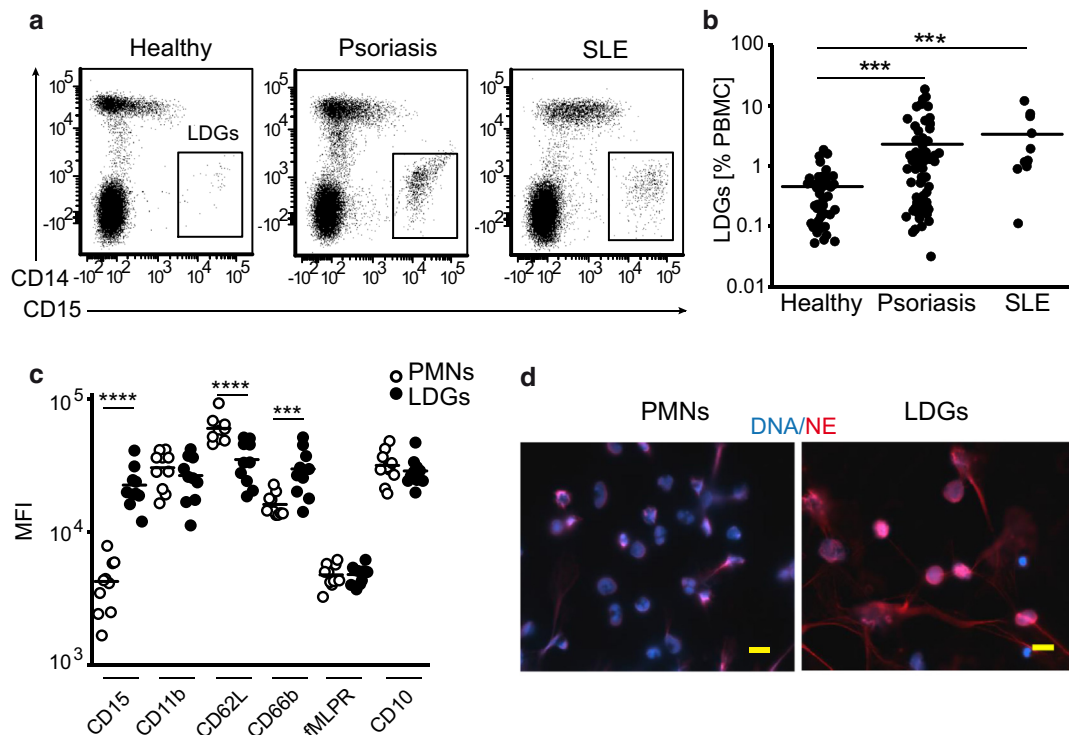


**Figure 2. Circulating LDGs are present at higher frequencies in psoriasis compared with normal donors and have the phenotypic and functional features of matured, activated, and pro-inflammatory neutrophils.** PBMCs were isolated from the blood of indicated donors and stained for LDGs and monocytes using anti-CD15 and anti-CD14 mAbs. The cells were then analyzed by flow cytometry. (a) Representative flow cytometry plots of the LDGs are shown. (b) Data are shown as the percentage of LDGs among PBMC. Lines indicate the mean value for each data set.  $n = 45, 70,$  and  $11$  for healthy, psoriasis, and SLE donors, respectively.  $***P < 0.001$ ; Kruskal-Wallis ANOVA, Dunn post hoc test. (c) Expression of the indicated molecules was evaluated on LDGs and PMNs from psoriasis patients by flow cytometry. Data are shown as the MFI among indicated antigen expression in autologous pairs of LDGs versus PMNs. Lines indicate the mean value for each data set;  $n = 10$  donors in each group.  $***P < 0.001$ ,  $****P < 0.0001$ ; two-way matched ANOVA; Sidak post hoc test. (d) Cell-sorted PMNs and LDGs were harvested on poly-L-lysine coated slides and incubated for 3 hours. Cells were then stained for NE (red), counterstained with Hoechst to detect DNA (blue), and examined by fluorescence microscopy. One representative dataset of at least three experiments is shown. Bar =  $10 \mu\text{m}$ . ANOVA, analysis of variance; LDG, low-density granulocyte; MFI, mean fluorescence intensity; PBMC, peripheral blood mononuclear cell; PMN, polymorphonuclear neutrophil; SLE, systemic lupus erythematosus.

cell activation, in agreement with other studies (Teague et al., 2019). Likewise, fluorescence microscopy revealed that a majority of LDGs possessed segmented nuclei, with a minority possessing ovoid nuclei (Figure 3c), suggesting a primarily mature status of these cells in psoriasis patients.

To assess the functional capacity of LDGs relative to autologous PMNs from psoriasis patients, both cell populations were tested for NET formation. In agreement with previous reports (Naik et al., 2015; Teague et al., 2019), LDGs displayed a higher ability than PMNs to spontaneously form NETs (Figure 2d and Supplementary Figure S1), indicative of a potentially augmented pathogenic capacity of LDGs compared with their PMN counterparts.

#### **LDGs and PMNs exhibit different staining for NE and SLPI but are roughly equal in NE and SLPI protein levels and NE proteolytic activity**

By flow cytometry, we next analyzed whether LDGs and PMNs differ in their levels of NE and SLPI, focusing on both cell surface and intracellular NE and SLPI. A small fraction of fixed LDGs showed a differential surface presentation of NE and SLPI compared with fixed autologous PMNs (Figure 3a). However, when the cells were fixed and then permeabilized

to target the intracellular NE and SLPI, the marked difference in the staining for NE and SLPI between a majority of LDGs and autologous PMNs was observed (Figure 3a). Thus, in subsequent experiments, we stained the permeabilized cells to target both cell surface and intracellular NE and SLPI. In addition to flow cytometry, immunohistochemistry also revealed that the LDGs exhibit much stronger staining for NE and lesser staining for SLPI, compared with the autologous PMNs (Figure 3b and c, respectively). Higher and weaker immunoreactivity to NE and SLPI were apparent when the LDGs were stained together with other cells in the PBMC fraction (Figure 3c) and after they were purified by cell sorting (Figure 3d). Whereas PMNs displayed NE and SLPI staining that was mostly restricted to a granular pattern, autologous LDGs showed more dispersed NE (Figure 3e). Targeting either NE or SLPI with three different Abs followed by flow cytometry analysis demonstrated similar staining patterns between autologous LDGs and PMNs, suggesting that these differences are independent of the staining Abs (Supplementary Figure S2).

We next quantified NE in lysates of PMNs and LDGs isolated from psoriasis patients by ELISA. As a control, we used autologous monocytes that do not express NE (Fouret et al., 1989) but are known to produce SLPI (Majchrzak-Gorecka



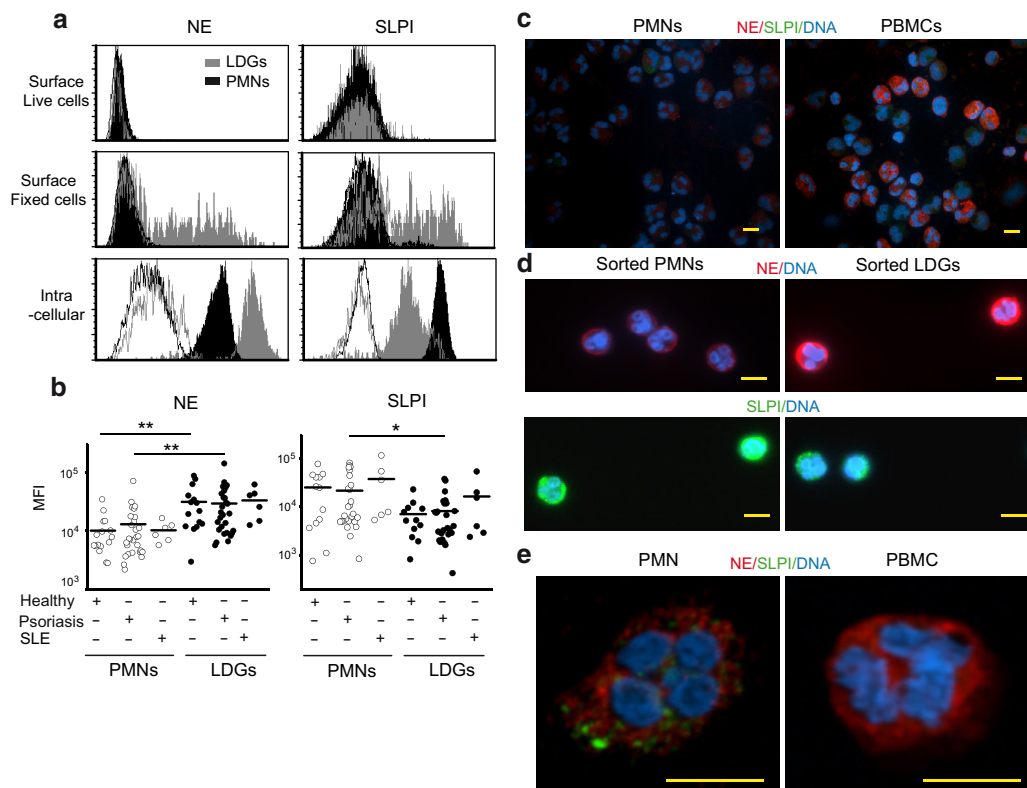


**Figure 3. LDGs have greater immunoreactivity for NE and weaker for SLPI relative to the autologous PMNs.** PBMCs and PMNs were isolated from blood and stained for LDGs and PMNs using anti-CD15 and anti-CD14 mAbs. (a) Expression of NE or SLPI was evaluated on live (upper panel), fixed (middle panel), or fixed and permeabilized (lower panel) LDGs (gray) and PMNs (black). Representative flow cytometry histogram plots of psoriasis patients are shown,  $n = 3$ . Open histograms indicate the respective staining controls. (b) Expression of NE or SLPI was evaluated on permeabilized LDGs and PMNs of indicated donors by flow cytometry. Lines indicate the mean value for each data set. Statistically significant differences between PMN and LDGs are indicated by asterisks (\*\* $P < 0.01$ , \* $P < 0.05$ ; Kruskal-Wallis analysis of variance, Dunn post hoc test). (c) Expression of NE and SLPI on PMNs and PBMCs from psoriasis donors was analyzed by immunohistochemistry,  $n = 5$ . (d) Expression of NE and SLPI on cell-sorted PMNs and LDGs from psoriasis donors was analyzed by fluorescence microscopy,  $n = 3$ . (e) Confocal microscopy images of NE and SLPI in PMNs and LDGs from a healthy donor. PMNs and LDGs were analyzed under the different acquisition settings (different exposure time) to best visualize the distribution of NE and SLPI.  $n = 3$ . Bar = 10  $\mu\text{m}$ . LDG, low-density granulocyte; MFI, mean fluorescence intensity; PBMC, peripheral blood mononuclear cell; PMN, polymorphonuclear neutrophil; SLE, systemic lupus erythematosus.

et al., 2016). There were no notable differences between autologous LDGs and PMNs in the total NE protein content (Figure 4a). Although SLPI levels were variable in leukocytes from different donors, they were likewise found to be comparable in autologous PMNs and LDGs on average (Figure 4b). Overall, these data suggest that the stronger staining of LDGs for NE and weaker staining for SLPI, in comparison to PMNs, cannot be attributed to the difference in cellular content of NE and SLPI.

Using an activity-based spectrometric assay, we next determined the enzymatic potential of NE in lysates of LDGs and PMNs sorted from psoriasis patients. On average, the LDGs and PMNs were found to contain similar levels of catalytically active NE, as indicated by the hydrolysis of a widely used chromogenic, synthetic peptide substrate, MeO-SucaAPVpNA. However, a trend toward reduced NE activity in LDGs (compared with autologous PMNs) was observed (Figure 4c). Similar results were obtained when the NE activity was measured in LDG and PMN lysates, using an energy transfer substrate (Abz-APEEIMRRQ-EDDnp), which is highly specific for NE (Figure 4d) (Korkmaz et al., 2008). These data indicate that the total levels of active NE are roughly similar in LDGs and PMNs.

#### Extra NE and SLPI epitopes in PMNs and LDGs are revealed in some individuals following the disruption of actin cytoskeleton dynamics

The staining heterogeneity for NE and SLPI observed could be caused by a difference in the accessibility of these antigens for detection with Abs. In resting PMNs, NE and SLPI are stored in primary and secondary granules, respectively. However, following neutrophil activation that results in NET formation, NE translocates to the nucleus, and SLPI likely follows (Zabieglo et al., 2015). Since interactions with the cytoskeleton may regulate NE and/or SLPI accessibility, we treated the PMNs and LDGs with latrunculin A or wiskostatin to inhibit actin polymerization. The treatment of PMNs resulted in much stronger staining for NE (Figure 5a) in approximately 67% of the donors, whereas the staining remained at a similar level in the other 33%. Moreover, in some donors, the treatment facilitated the translocation of NE to the nucleus (Figure 5b). In these cells, SLPI was not detectable (Figure 5b). Likewise, in approximately 67% of the donors, the LDGs showed reduced staining for NE following treatment with latrunculin; a stronger staining for SLPI was observed following treatment with latrunculin (approximately 50% of donors)

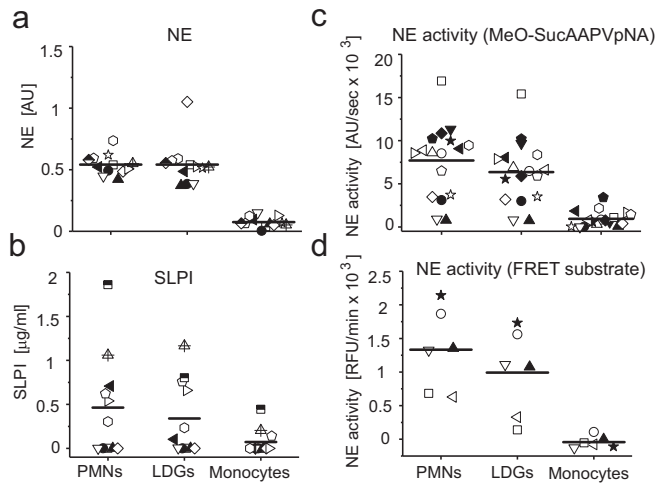


**Figure 4. Psoriasis LDGs and PMNs have similar protein levels of NE and SLPI and do not differ significantly in their NE activity.** PMNs (CD15<sup>+</sup>, CD14<sup>-</sup>) were sorted from PMN fractions, whereas LDGs (CD15<sup>+</sup>, CD14<sup>-</sup>) and monocytes (CD14<sup>+</sup>, CD15<sup>-</sup>) were sorted from the PBMC fraction of psoriasis patients. (a) NE and (b) SLPI protein levels were assessed in the cell lysates by ELISA. Lines indicate the mean value for each data set, n = 12. (c) NE enzymatic activity in cell lysates was measured by a MeO-SucAAPVpNA hydrolysis assay, n = 17, (d) or by fluorimetry, using the fluorescence resonance energy transfer substrate, Abz-APEEIMRRQ-EDDnp, n = 6. Lines indicate the mean value for each data set. Each patient is marked by a different symbol in each panel and across panels. AU, absorbance units; FRET, fluorescence resonance energy transfer; LDG, low-density granulocyte; PMN, polymorphonuclear neutrophil; RFU, relative fluorescence units.

(Figure 5b) and wiskostatin (approximately 67% of donors). Thus, the apparent presence of NE or SLPI in both neutrophil populations could be unmasked by forced changes in cytoskeleton dynamics.

We next asked if the inhibition of actin polymerization in PMNs results in PMNs that functionally resemble LDGs. We tested this using NET formation as a readout, because the LDGs of both psoriasis and healthy donors (Figure 2 and Supplementary Figure S1) spontaneously form more NETs. On average, latrunculin- or wiskostatin-treated PMNs appeared to increase their tendency to release NETs, in line with a previous report (Cervantes-Luevano et al., 2018).

#### LDGs and PMNs differ in their chemotactic attributes

Cytoskeleton remodeling is critically involved in cell migration. LDGs and PMNs may use the interaction between actin cytoskeleton and NE and/or SLPI to differentially control cell movement. Therefore, we next determined whether these neutrophil populations exhibit differences in chemotactic response. To mimic the skin environment associated with neutrophil recruitment to inflamed skin, we used skin extracts prepared from biopsies of lesional skin of psoriasis patients. The chemoattractant N-formylmethionyl-leucyl-phenylalanine (fMLP) and the psoriasis-associated chemokine CXCL1 (Li et al., 2014) were used as positive controls, whereas chemotaxis medium was used as a negative control. When autologous PBMCs and PMNs isolated from the blood of psoriasis donors were assessed in a standard Transwell chemotaxis assay, the LDGs showed a trend for a better chemotactic response to the skin extracts compared with

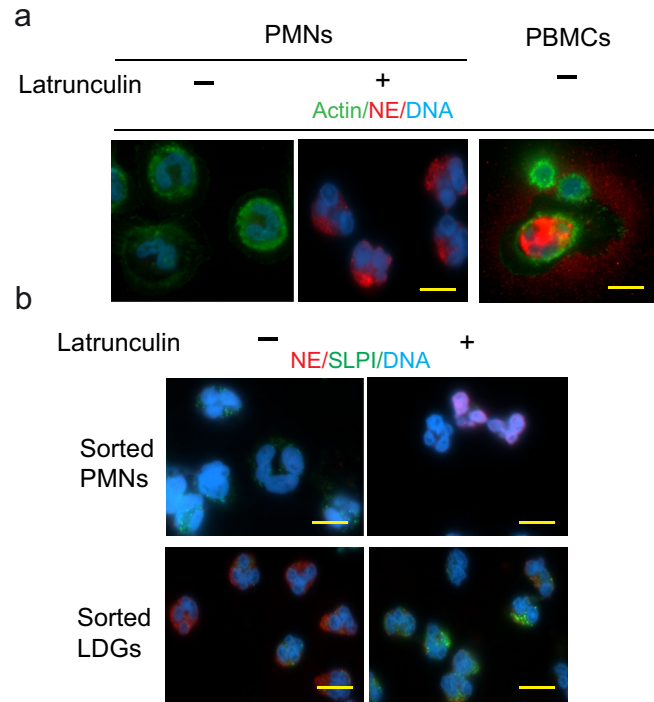


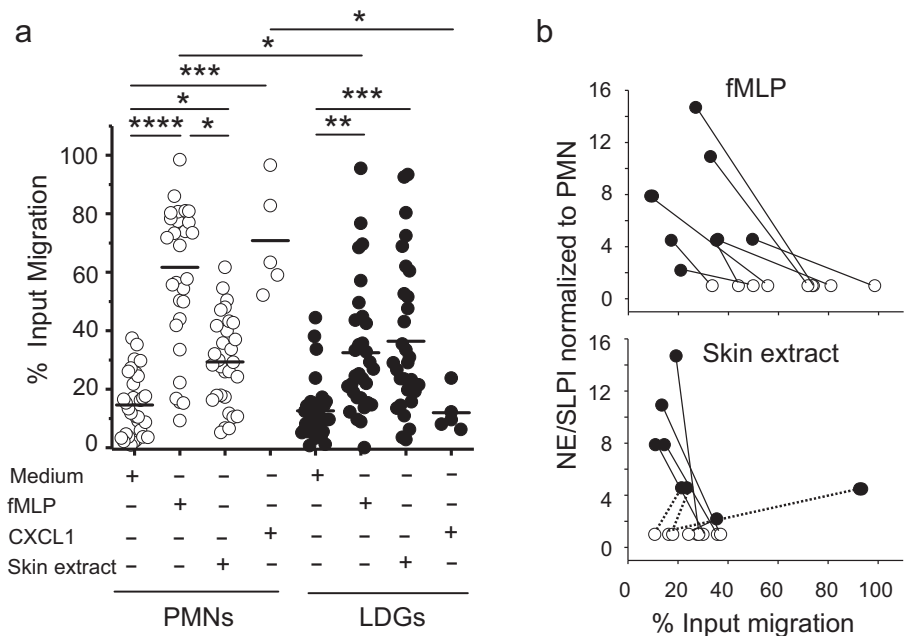
**Figure 5. Disruption of the actin cytoskeleton alters the immunoreactivity for NE and SLPI in neutrophils and facilitates the translocation of NE to the nucleus in PMNs.** (a) Circulating PMNs and PBMCs from a healthy donor and (b) negatively sorted PMNs and LDGs from a psoriasis patient were treated with latrunculin A to disrupt the actin cytoskeleton. Control cells were treated with vehicle (-). (a) Cells were then stained with phalloidin to visualize F-actin (green) and for NE (red), (b) or for NE (red) and SLPI (green). Cells were examined by fluorescence microscopy. Data are representative of four independent experiments. LDG, low-density granulocyte; PBMC, peripheral blood mononuclear cell; PMN, polymorphonuclear neutrophil.

the PMNs. In contrast, fMLP appeared to attract a higher number of PMNs than LDGs (Supplementary Figure S3). Since other cells present in PBMC fractions might selectively influence the chemotactic response of LDGs, we next labeled PMNs with carboxyfluorescein succinimidyl ester, and then we mixed carboxyfluorescein succinimidyl ester-labeled PMNs with PBMCs, followed by the chemotaxis assay. Unlabeled PMNs and carboxyfluorescein succinimidyl ester-labeled PMNs showed a similar relative response either to skin extracts or fMLP; the combined chemotactic response of both unlabeled and carboxyfluorescein succinimidyl ester-labeled PMNs and LDGs is shown in Figure 6a. Overall, the LDGs were found to respond better to skin extracts but migrate significantly less efficiently to fMLP and CXCL1 when compared with the PMNs. These experiments confirmed that the difference in migration is mainly a result of an intrinsic feature of these neutrophil populations.

The inhibition of NE activity by synthetic inhibitor GW311616A, which penetrates cell membranes and thus targets intracellular NE, reduced the migration index of PMNs and LDGs by 30–40% on average (Supplementary Figure S4). These data suggest that the migratory capacity of PMNs and LDGs depends on active NE. Since the LDGs from different donors differed markedly in their migratory potential, most notably to skin extracts (Figure 6a), we next asked

**Figure 6. LDGs and PMNs from psoriasis donors differ in their chemotactic response.**

(a) PMNs and LDGs (CD15+ PBMCs) migration to the fMLP, CXCL1, or psoriasis skin extracts was assessed by an in vitro Transwell chemotaxis assay. Migration to media only is shown as negative control.  $n = 19$  donors. Data points mainly represent the values of two samples from each donor: For PMNs, CFSE-unlabeled, and CFSE-labeled PMNs that were mixed with PBMCs; for LDGs, PBMCs, and PBMCs that were mixed with CFSE-labeled PMNs. The mean value in each group is shown. Statistically significant differences between the groups are indicated by asterisks (\* $P < 0.05$ , \*\* $P < 0.01$ , \*\*\* $P < 0.001$ , \*\*\*\* $P < 0.0001$ ; two-way Kruskal-Wallis analysis of variance, Dunn post hoc test). (b) Chemotaxis of autologous LDGs and PMNs to fMLP and skin extracts is shown as a function of the NE to SLPI index in LDGs normalized to the NE to SLPI index in PMNs. CFSE, carboxyfluorescein succinimidyl ester; fMLP, N-formylmethionyl-leucyl-phenylalanine; LDG, low-density granulocyte; PBMC, peripheral blood mononuclear cell; PMN, polymorphonuclear neutrophil.



whether this correlated with staining for NE and SLPI. For this analysis, the chemotaxis index of autologous PMNs and LDGs is shown as a function of the NE/SLPI staining ratio in the skin extracts-stimulated and fMLP-stimulated neutrophils (Figure 6b). LDGs displayed diverse NE/SLPI ratios, ranging from 2-fold to 16-fold above the autologous PMNs. The LDGs consistently migrated less efficiently to fMLP, despite the difference in the NE/SLPI ratio. However, the migration to skin extracts revealed two migration patterns of the LDGs in relation to NE/SLPI index. The LDGs that displayed the lowest NE/SLPI ratio (2–5 $\times$ ) appeared to respond better, whereas those with higher NE/SLPI ratios (>5 $\times$  up to 16 $\times$ ) migrated less efficiently to skin extracts compared with autologous PMNs.

## DISCUSSION

Here, we report the previously uncharacterized differences in staining for NE and SLPI in LDGs in comparison to autologous PMNs (Figure 3). Although this phenotype was not unique to individuals suffering from psoriasis, it is likely to primarily have a functional impact on patients with autoimmune diseases, such as psoriasis, which are characterized by a high prevalence of LDGs.

The augmented and reduced staining for NE and SLPI in the LDGs suggested that frequent NETs formation by LDGs might result from elevated NE activity that has not been fully inhibited by SLPI. We found that neither the quantity nor bioactivity of total NE appear to be significantly altered in LDGs. However, cell lysis, which was required for the measurement of intracellular NE activity, may disrupt the interaction of NE with its intracellular partners and influence its functional state. Because SLPI is a reversible inhibitor of NE, it may be particularly well-suited to dynamically control NE activity. However, the transient

nature of interactions between NE and SLPI can be easily reversed by cell lysis conditions.

Differential staining for NE and SLPI in LDGs and PMNs was mainly localized in the cytoplasm (Figure 3). As such, the data suggested that the partial release of NE to the cytosol, with possible binding to the cytoskeleton and/or other cytosol components, may be responsible for the differences in the NE staining between LDGs and PMNs. For example, the localized enrichment of NE on the cytoskeleton and/or better availability of the NE immunoreactive epitopes could be responsible for the stronger staining of LDGs for NE. Our staining data support this scenario, since in contrast to PMNs, the LDGs exhibited more dispersed NE staining patterns in the cytoplasm, suggesting some release of granule content. The SLPI's level of detection inversely correlated with NE in the neutrophil populations. The LDGs may be more restricted than PMNs in mobilizing SLPI from secondary granules, resulting in a distinct level or order of SLPI presentation to cytosolic substrates and less effective control of the NE activity. This is in line with the appearance of additional NE and SLPI epitopes in PMNs and LDGs of some patients as a result of the forced changes in actin cytoskeleton dynamics.

With respect to the NE and/or SLPI staining, skin-infiltrating neutrophils overlapped to some extent with the circulating PMNs and/or LDGs. Moreover, in the in vitro chemotaxis assay, the LDGs showed an elevated tendency to migrate to psoriasis skin extracts on average, whereas the PMNs exhibited significantly more robust migration to fMLP and CXCL1 (Figure 6a). These data suggest that both neutrophil populations are likely to be recruited into the inflamed skin but possibly localized to different skin regions, owing to a differential migratory response. This would be consistent with the segregation of neutrophils that exhibit



a different NE and/or SLPI staining pattern to different skin niches (Figure 1). For example, fMLP attracted significantly more PMNs than LDGs, despite comparable levels of cell surface fMLP receptors in PMNs and LDGs (Figures 6 and 2, respectively). PMNs, by following the gradient of peptides with formyl methionine (which mimics bacterial peptides), are more likely to localize to upper skin regions where neutrophils may acquire bacteria or bacterial products coming from the skin surface (Kwiecien et al., 2019). However, it is also possible that neutrophils in the skin differentially employ active NE to migrate and localize to different skin niches, irrespective of their LDGs and/or PMNs features.

Cytosolic NE was previously proposed to regulate neutrophil migration. In these studies, NE interference with actin dynamics was suggested to disable the cell movement and confine "NETting" neutrophils to the NET trigger site (Metzler et al., 2014). Our data suggest that a higher cytosolic content of NE, as seen in LDGs compared with autologous PMNs, does not necessarily result in neutrophil immobilization, as some LDGs were well-fitted to migrate to psoriasis skin extracts. However, this may depend on the level of unrestrained NE in the cytosol, as the high NE to SLPI index in LDGs appeared to render these cells less able to migrate to both fMLP and skin extracts (Figure 6).

The translocation of NE from the granules to the cytosol can occur in response to neutrophil activation, whereas in LDGs this may be a result of leaky primary granules at steady state. This would be reminiscent of NE translocation to the cytosol in aging neutrophils, which use NE to cleave gasdermin D and expedite neutrophil death (Kambara et al., 2018). Thus, the presence of NE in the cytosol appears to be a common feature of different functional states, leading to neutrophil migration, immobilization, or death, with the type of neutrophil inducer likely evoking a different response. However, the permanent localization of NE in the cytosol may endow LDGs with some pathogenic features, such as the ability to respond in a less-controlled manner or with a lower threshold to different stimuli.

In summary, the staining for NE and SLPI revealed heterogeneity among either skin-infiltrating or circulating neutrophils in psoriasis patients. The difference is likely owing to higher and lower cytosolic content of NE and SLPI, respectively, and/or different arrangement of these molecules in the cytoplasm in LDGs compared with PMNs. LDGs and PMNs also differ in their chemotactic responses. Taken together, these results are consistent with a model in which cytosol-exposed NE, not fully inhibited by SLPI, contributes to distinct functional and migratory behavior of LDGs in comparison to the PMNs. Their capacity to differentially respond to chemotaxis signals impacts the distribution of these cells in the skin, allowing the LDGs and PMNs to be triggered by distinct signals. LDGs respond in an exaggerated manner to cutaneous stimuli, notably by an augmented release of NETs, leading to skin pathology.

## MATERIALS AND METHODS

### Human samples

Human samples were collected from individuals who were fully informed and had consented (written consent was obtained from

patients), and human studies were approved by the Jagiellonian University Institutional Bioethics Committee. In total, 116 psoriasis patients (age  $38.1 \pm 12.8$ ; male:female 72:44), 12 SLE patients (age  $40.82 \pm 14$ , male:female 2:10), and 63 healthy individuals (age  $31.7 \pm 7.7$ ; male:female 27:36) were enrolled in the study. The severity of the psoriatic skin lesions was assessed according to the Psoriasis Area Severity Index score (minimum, 0 points; maximum, 72 points) and ranged from 1.9 to 62 (mean  $\pm$  standard deviation:  $16.4 \pm 9.7$ ). The SLE disease activity was assessed by the SLE disease activity index 2000 (Gladman et al., 2002).

### Isolation of the LDGs and PMNs

Blood was collected into sodium citrate collection tubes and subjected to the isolation of PMNs and LDGs within 1.5 hours of draw. PBMCs and PMNs were isolated by a density gradient 1,077 g/ml centrifugation using Pancoll (PANBiotech, Aidenbach, Germany). LDGs, identified as CD15+ and CD14-, were purified from the PBMCs by cell sorting (MoFlowTMXDP, Beckman Coulter, Brea, CA). Alternatively, LDGs were enriched by negative sorting using an EasySep Human Neutrophil Enrichment Kit (STEMCELL Technologies, Vancouver, Canada). The purity of the cell- and magnetically-sorted LDGs was typically around 90% and 50%, respectively.

PMNs were recovered from the corresponding erythrocyte fraction of the Pancoll gradient as previously described (Skrzeczynska-Moncznik et al., 2012). Where indicated, PMNs were further purified by cell sorting using mAbs directed against CD14 and CD15. The PMNs were routinely > 98% pure.

### Flow cytometry

For the staining for NE and SLPI, the PMNs and PBMCs were first fixed with 3.7% formaldehyde and permeabilized with 0.1% saponin in phosphate buffered saline. The cells were incubated with primary antibodies—polyclonal rabbit-anti-NE IgG (Athens Research and Technology, Athens, GA) and/or monoclonal-biotin-mouse-anti-SLPI (Abcam, Cambridge, United Kingdom) followed by secondary antibodies; allophycocyanin-F(ab)2 goat-antirabbit IgG (Jackson ImmunoResearch, West Grove, PA) and phycoerythrin- or allophycocyanin-streptavidin (eBioscience, San Diego, CA or BD Pharmingen, San Jose, CA). Where indicated, the cells were stained without the fixation or permeabilization step. The same primary Abs for NE and SLPI were used across all the assays, unless otherwise indicated. Flow cytometry was performed on an LSRII (BD Biosciences, San Jose, CA), and the data were analyzed using the DIVA and FCS Express software.

### Immunohistochemistry

Frozen 6- $\mu$ m sections were prepared from skin biopsies and stained as previously described (Zabieglo et al., 2015). Purified PMNs, LDGs, or PBMCs were seeded on poly-L-lysine coated slides ( $2-5 \times 10^5$  cells per coverslip) and incubated at 37 °C, 5% carbon dioxide for 30 minutes in serum-free RPMI. When indicated, the cells were incubated for 3 hours to assess their ability to form NETs or treated with 1  $\mu$ M latrunculin A (Invitrogen, Carlsbad, CA) or 100 nM wiskostatin (Sigma-Aldrich, St. Louis, MO) for 30 minutes. The cells were then fixed with 3.7% formaldehyde, treated with 0.1% saponin in phosphate buffered saline, and stained for NE, SLPI, and DNA (Zabieglo et al., 2015). For cytoskeleton detection, the cells were permeabilized with 1% Triton X100 (ICN, Costa Mesa, CA) and stained with phalloidin-AlexaFluor488 (Invitrogen, Carlsbad, CA) to visualize actin. Images were captured with a fully motorized fluorescence or

confocal microscope (Nikon, Eclipse, Tokyo, Japan) and analyzed by NIS elements software (Nikon).

### Data availability statement

The data that support the findings of this study are available from the corresponding author upon reasonable request.

### ORCIDs

Joanna Skrzeczynska-Moncznik: <https://orcid.org/0000-0001-5566-1453>  
Katarzyna Zabieglo: <https://orcid.org/0000-0003-4708-7054>  
Oktawia Osiecka: <https://orcid.org/0000-0001-5538-5313>  
Agnieszka Morytko: <https://orcid.org/0000-0002-8741-7356>  
Piotr Brzoza: <https://orcid.org/0000-0003-0516-3266>  
Lukasz Drozd: <https://orcid.org/0000-0003-3157-9417>  
Monika Kapinska-Mrowiecka: <https://orcid.org/0000-0001-8184-9265>  
Brice Korkmaz: <https://orcid.org/0000-0002-5159-8706>  
Maciej Pastuszcak: <https://orcid.org/0000-0001-7241-9685>  
Joanna Kosalka-Wegiel: <https://orcid.org/0000-0003-1013-2253>  
Jacek Musial: <https://orcid.org/0000-0002-0955-1808>  
Joanna Cichy: <https://orcid.org/0000-0002-0552-8344>

### CONFLICT OF INTEREST

The authors state no conflict of interest.

### ACKNOWLEDGMENTS

We would like to thank former visiting Fulbright U.S. researcher James Jung for his English editing.

This work was supported by grants from Polish National Science Center UMO-2011/02/A/NZ5/00337 and UMO-2017/25/B/NZ6/01003 (to JC). This work was also supported by European COST Action BM1404 Mye-EUNITER ([www.mye-euniter.eu](http://www.mye-euniter.eu)).

### AUTHOR CONTRIBUTIONS

Conceptualization: JC, JSM; Formal Analysis: JSM, PB; Funding Acquisition: JC; Investigation: JSM, KZ, OO, AM, PB, LD; Methodology: JSM, BK; Project Administration: JC; Resources: MKM, BK, MP, JKW, JM; Supervision: JC; Writing – Original Draft: JC; Writing – Review and Editing: JC

### SUPPLEMENTARY MATERIAL

Supplementary material is linked to the online version of the paper at [www.jidonline.org](http://www.jidonline.org), and at <https://doi.org/10.1016/j.jid.2019.12.015>.

### REFERENCES

- Bennett L, Palucka AK, Arce E, Cantrell V, Borvak J, Banchereau J, et al. Interferon and granulopoiesis signatures in systemic lupus erythematosus blood. *J Exp Med* 2003;197:711–23.
- Carmona-Rivera C, Kaplan MJ. Low-density granulocytes: a distinct class of neutrophils in systemic autoimmunity. *Semin Immunopathol* 2013;35:455–63.
- Cervantes-Luevano KE, Caronni N, Castiello MC, Fontana E, Piperno GM, Naseem A, et al. Neutrophils drive type I interferon production and auto-antibodies in patients with Wiskott-Aldrich syndrome. *J Allergy Clin Immunol* 2018;142:1605–17.e4.
- Denny MF, Yalavarthi S, Zhao W, Thacker SG, Anderson M, Sandy AR, et al. A distinct subset of proinflammatory neutrophils isolated from patients with systemic lupus erythematosus induces vascular damage and synthesizes type I IFNs. *J Immunol* 2010;184:3284–97.
- Fouré P, du Bois RM, Bernaudin JF, Takahashi H, Ferrans VJ, Crystal RG. Expression of the neutrophil elastase gene during human bone marrow cell differentiation. *J Exp Med* 1989;169:833–45.
- Gladman DD, Ibañez D, Urowitz MB. Systemic lupus erythematosus disease activity index 2000. *J Rheumatol* 2002;29:288–91.
- Hacbarth E, Kajdacsy-Balla A. Low density neutrophils in patients with systemic lupus erythematosus, rheumatoid arthritis, and acute rheumatic fever. *Arthritis Rheum* 1986;29:1334–42.
- Henry CM, Sullivan GP, Clancy DM, Afonina IS, Kulms D, Martin SJ. Neutrophil-derived proteases escalate inflammation through activation of IL-36 family cytokines. *Cell Rep* 2016;14:708–22.

- Kambara H, Liu F, Zhang X, Liu P, Bajrami B, Teng Y, et al. Gasdermin D exerts anti-inflammatory effects by promoting neutrophil death. *Cell Rep* 2018;22:2924–36.
- Korkmaz B, Attucci S, Juliano MA, Kalupov T, Jourdan ML, Juliano L, et al. Measuring elastase, proteinase 3 and cathepsin G activities at the surface of human neutrophils with fluorescence resonance energy transfer substrates. *Nat Protoc* 2008;3:991–1000.
- Kwiecien K, Zegar A, Jung J, Brzoza P, Kwitniewski M, Godlewska U, et al. Architecture of antimicrobial skin defense. *Cytokine Growth Factor Rev* 2019;49:70–84.
- Lambert S, Hambro CA, Johnston A, Stuart PE, Tsoi LC, Nair RP, et al. Neutrophil extracellular traps induce human Th17 cells: effect of psoriasis-associated TRAF3IP2 genotype. *J Invest Dermatol* 2019;139:1245–53.
- Lande R, Ganguly D, Facchinetti V, Frasca L, Conrad C, Gregorio J, et al. Neutrophils activate plasmacytoid dendritic cells by releasing self-DNA-peptide complexes in systemic lupus erythematosus. *Sci Transl Med* 2011;3:73ra19.
- Li N, Yamasaki K, Saito R, Fukushi-Takahashi S, Shimada-Omori R, Asano M, et al. Alarmin function of cathelicidin antimicrobial peptide LL37 through IL-36gamma induction in human epidermal keratinocytes. *J Immunol* 2014;193:5140–8.
- Lin AM, Rubin CJ, Khandpur R, Wang JY, Riblett M, Yalavarthi S, et al. Mast cells and neutrophils release IL-17 through extracellular trap formation in psoriasis. *J Immunol* 2011;187:490–500.
- Majchrzak-Gorecka M, Majewski P, Grygier B, Murzyn K, Cichy J. Secretory leukocyte protease inhibitor (SLPI), a multifunctional protein in the host defense response. *Cytokine Growth Factor Rev* 2016;28:79–93.
- Metzler KD, Goosmann C, Lubojemska A, Zychlinsky A, Papayannopoulos V. A myeloperoxidase-containing complex regulates neutrophil elastase release and actin dynamics during NETosis. *Cell Rep* 2014;8:883–96.
- Naik HB, Natarajan B, Stansky E, Ahlman MA, Teague H, Salahuddin T, et al. Severity of Psoriasis Associates with aortic vascular inflammation detected by FDG PET/CT and neutrophil activation in a prospective observational study. *Arterioscler Thromb Vasc Biol* 2015;35:2667–76.
- Nicolás-Ávila JÁ, Adrover JM, Hidalgo A. Neutrophils in homeostasis, immunity, and cancer. *Immunity* 2017;46:15–28.
- Papayannopoulos V, Metzler KD, Hakkim A, Zychlinsky A. Neutrophil elastase and myeloperoxidase regulate the formation of neutrophil extracellular traps. *J Cell Biol* 2010;191:677–91.
- Sagiv JY, Michaeli J, Assi S, Mishalian I, Kisos H, Levy L, et al. Phenotypic diversity and plasticity in circulating neutrophil subpopulations in cancer. *Cell Rep* 2015;10:562–73.
- Scapini P, Marini O, Tecchio C, Cassatella MA. Human neutrophils in the saga of cellular heterogeneity: insights and open questions. *Immunol Rev* 2016;273:48–60.
- Skrzeczynska-Moncznik J, Włodarczyk A, Zabieglo K, Kapinska-Mrowiecka M, Marewicz E, Dubin A, et al. Secretory leukocyte proteinase inhibitor-competent DNA deposits are potent stimulators of plasmacytoid dendritic cells: implication for psoriasis. *J Immunol* 2012;189:1611–7.
- Teague HL, Varghese NJ, Tsoi LC, Dey AK, Garshick MS, Silverman JJ, et al. Neutrophil subsets, platelets, and vascular disease in psoriasis. *JACC Basic Transl Sci* 2019;4:1–14.
- Villanueva E, Yalavarthi S, Berthier CC, Hodgins JB, Khandpur R, Lin AM, et al. Netting neutrophils induce endothelial damage, infiltrate tissues, and expose immunostimulatory molecules in systemic lupus erythematosus. *J Immunol* 2011;187:538–52.
- Zabieglo K, Majewski P, Majchrzak-Gorecka M, Włodarczyk A, Grygier B, Zegar A, et al. The inhibitory effect of secretory leukocyte protease inhibitor (SLPI) on formation of neutrophil extracellular traps. *J Leukoc Biol* 2015;98:99–106.



This work is licensed under a Creative Commons Attribution-NonCommercial-NoDerivatives 4.0 International License. To view a copy of this license, visit <http://creativecommons.org/licenses/by-nc-nd/4.0/>



## SUPPLEMENTARY MATERIALS AND METHODS

### Low-density granulocytes (LDGs) and polymorphonuclear neutrophils (PMNs) immunophenotyping

Peripheral blood mononuclear cells and PMNs isolated from psoriasis patients were stained with the following directly-conjugated monoclonal mouse antihuman antibodies: anti-CD15, CD14, CD11b, CD66b, and CD10 (all from BioLegend, San Diego, CA); anti-CD62L (eBioscience, San Diego, CA), anti-fMLPR (Miltenyi Biotec, Bergisch Gladbach, Germany), or mouse isotype controls. Flow cytometry was performed on an LSRII (BD Biosciences, San Jose, CA), and the data were analyzed using the DIVA and FCS Express software.

### ELISA

The levels of NE and SLPI were quantified in lysates of PMNs and LDGs using direct and sandwich ELISA, respectively. A total of  $2 \times 10^5$  cells were sorted into 50  $\mu$ l RIPA lysis buffer (Sigma-Aldrich, Saint Louis, MO). The cell lysates were collected and stored at  $-20^\circ\text{C}$  until used.

### Measurement of enzymatic activity

A total of  $5 \times 10^4$  cells were sorted into 50  $\mu$ l of 0.1% hexadecyltrimethylammonium bromide (Sigma-Aldrich) and incubated at  $37^\circ\text{C}$  for 15 minutes. NE activity was assayed in a colorimetric test using N-methoxysuccinyl-Ala-Ala-Pro-Val p-nitroanilide, (MeO-SucAAPVpNA) (Sigma-Aldrich) as a substrate. The absorbance was measured for at least 30 minutes using a microplate reader (Tecan Infinite M200, Mannedorf, Switzerland). The enzyme activity was expressed as an increase in absorbance at 405 nm per sec (area OD/sec).

Alternatively, NE activity were measured with the fluorescence resonance energy transfer substrate, Abz-APEEIMRRQ-EDDnp, using a microplate reader (Tecan Infinite M200) with

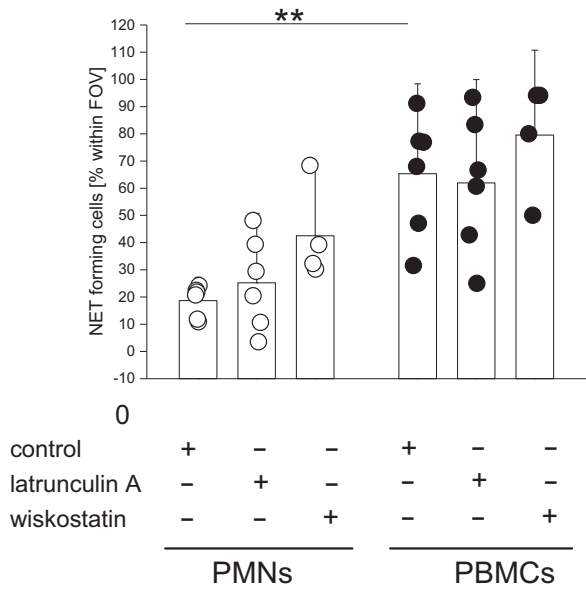
excitation 320 nm and emission 420 nm for 20 minutes at  $37^\circ\text{C}$ . The gain value was fixed at 100 for all the experiments allowing relative fluorescence units comparison.

### Preparation of skin extracts

Excisional biopsies were taken from the lesional skin of psoriasis patients. Skin samples were immediately minced in RPMI 1640 supplemented with 10% of fetal calf serum at 50 mg skin per 1 ml medium, followed by incubation for 6 hours at  $37^\circ\text{C}$ . Extracts were filtered through a 0.45  $\mu$ m cell strainer and stored at  $-80^\circ\text{C}$  until used.

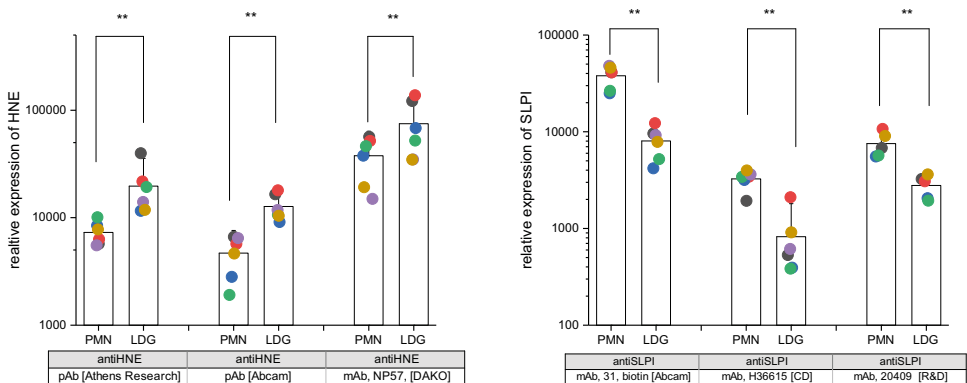
### Chemotaxis assay

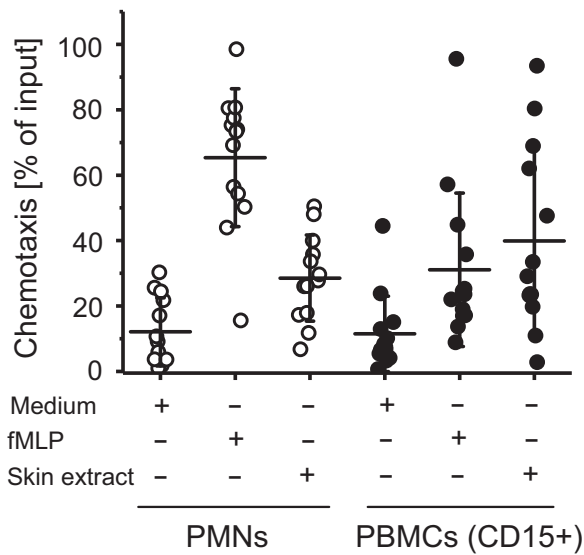
Neutrophil populations were tested in an in vitro chemotaxis assay. A volume of 100  $\mu$ l of cells ( $3 \times 10^5$  cells/well) was added to the top well of 3  $\mu$ m pore Transwell inserts (Costar, Sigma-Aldrich, Saint Louis, MO) and chemoattractants, 1 nM N-formylmethionyl-leucyl-phenylalanine, 50 ng/ml human CXCL1, skin extracts 1:10 (v:v) were added to the bottom well in a 600  $\mu$ l volume. In some experiments, the cells were preincubated with 20  $\mu$ M elastase inhibitor GW311616A (MedChemExpress, Princeton, New Jersey) for 30 minutes. Migration was assayed for 1.5 hours at  $37^\circ\text{C}$ . The inserts were then removed, and cells that had migrated through the filter to the lower chamber were collected, stained with anti-CD15 and CD14 mAbs, and counted by flow cytometry. In some experiments, the PMNs were first labeled with 62.5 nM CellTrace Carboxyfluorescein succinimidyl ester (ThermoFischer Scientific, Waltham, Massachusetts) for 20 minutes in phosphate buffered saline. Carboxyfluorescein succinimidyl ester-labeled PMNs were then mixed with autologous PBMCs at a 1:9 ratio.



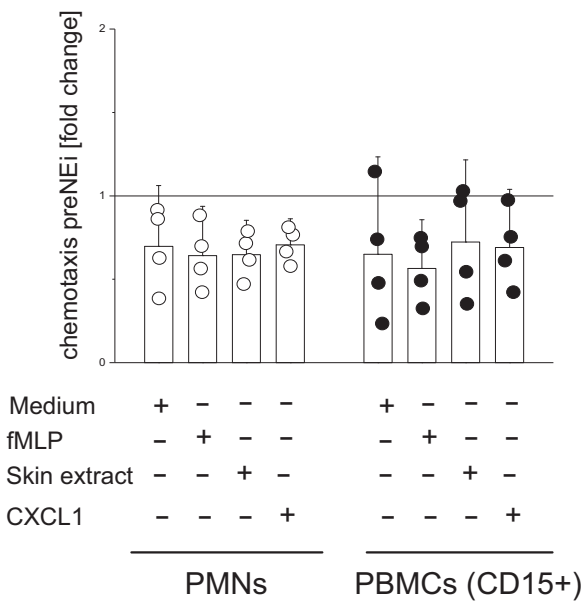
**Supplementary Figure S1. PMNs with a disrupted actin skeleton resemble autologous LDGs to some degree in the ability to spontaneously form NETs.** PMNs and PBMCs from healthy donors were treated for 30 minutes with wiskostatin or lantrunculin A, followed by staining for NE, SLPI, and DNA, and analysis by fluorescence microscopy. NETs were manually quantified from 10 randomized high-powered fields per sample and are expressed as the percentage of total cells. n = 4–6. Each data point represents one experiment, and bars indicate the mean value ± standard deviation in each group. \*\**P* < 0.001 by an analysis of variance followed by a Tukey post hoc test. FOV, field of view; NET, neutrophil extracellular trap; PBMC, peripheral blood mononuclear cell; PMN, polymorphonuclear neutrophil.

**Supplementary Figure S2. Difference in the NE and SLPI staining pattern between autologous PMNs and LDGs is revealed by different NE- and SLPI-specific Abs.** Peripheral blood mononuclear cells and PMNs were isolated from blood and stained for LDGs and PMNs using anti-CD15 and anti-CD14 mAbs. The expression of NE or SLPI was evaluated using the indicated anti-HNE and anti-SLPI Abs followed by secondary antibodies; allophycocyanin-F(ab)2 fragment goat-antirabbit IgG (Jackson ImmunoResearch) or allophycocyanin-goat antimouse IgG (Abcam, Cambridge, United Kingdom) and phycoerythrin-streptavidin (eBioscience, San Diego, CA or BD Pharmingen). Each data point represents one experiment, and bars indicate the mean value ± standard deviation in each group. \*\**P* < 0.01 by a *t*-test or Mann-Whitney test. LDG, low-density granulocyte; pAb, polyclonal antibody; PMN, polymorphonuclear neutrophil.





**Supplementary Figure S3. Chemotactic response of psoriasis blood-derived neutrophils.** PMNs and PBMCs were purified from the blood of psoriasis patients. The chemotactic responses of the cells to the indicated triggers were then assayed by in vitro Transwell chemotaxis assay. After 1.5 hours, the input and migratory cells were stained with anti-CD15 antibodies, to count neutrophils in either PMNs or PBMCs fraction.  $n = 10$ . Each data point represents one patient. The mean value  $\pm$  standard deviation in each group is shown. fMLP, N-formylmethionyl-leucyl-phenylalanine; PBMC, peripheral blood mononuclear cell; PMN, polymorphonuclear cell.



**Supplementary Figure S4. NE inhibitor lowers the chemotaxis index in PMNs and LDGs.** PMNs and LDGs (CD15<sup>+</sup> PBMCs) were treated with NEi or vehicle for 30 minutes. Cell migration to the fMLP, CXCL1, psoriasis skin extracts, or media only was assessed by an in vitro Transwell chemotaxis assay,  $n = 4$  donors. Data points represent the values of two samples from each donor. Each data point represents one patient. The mean value  $\pm$  standard deviation in each group is shown. fMLP, N-formylmethionyl-leucyl-phenylalanine; LDG, low-density granulocyte; NEi, synthetic inhibitor GW311616A; PBMC, peripheral blood mononuclear cell; PMN, polymorphonuclear cell.